Large amplitude forced vibration of functionally graded nano-composite plate with piezoelectric layers resting on nonlinear elastic foundation

Ali A. Yazdi*

Department of Mechanical Engineering, Quchan University of Technology, P. O. Box 94717-84686, Quchan, Iran

Abstract. This paper presents a study of geometric nonlinear forced vibration of carbon nano-tubes (CNTs) reinforcement composite plates on nonlinear elastic foundations. The plate is bonded with piezoelectric layers. The von Karman geometric nonlinearity assumptions with classical plate theory are employed to obtain the governing equations. The Galerkin and homotopy perturbation method (HPM) are utilized to investigate the effect of carbon nano-tubes volume fractions, large amplitude vibrations, elastic foundation parameters, piezoelectric applied voltage on frequency ratio and primary resonance. The results indicate that the carbon nano-tube volume fraction, applied voltage and elastic foundation parameters have significant effect on the hardening response of carbon nanotubes reinforced composite (CNTRC) plates.

Keywords: nonlinear forced vibration; carbon nano-tube; elastic foundation, Homotopy Perturbation method

1. Introduction

Nanocomposite plates and shells of various constructions have been used widely as new promising structural components into industry. The extraordinary and high aspect ratios of carbon nano-tubes (CNT) provide them as an alternative way to improve the properties of polymers and stiffness of structural elements. These novel properties have been prompted the researchers to consider the prospect of using carbon nano tubes in reinforcing the composite materials. Since the discovery of carbon nano-tubes by Iijima (1991), the application of these materials was extended widely in the researchers investigations regarding vibration and buckling response of composite structures.

Mirzaei and Kiani (2016) have studied the free vibration response of plate with cutout that was reinforced with CNT. They used the first shear deformation theory to obtain the equation of motion. Their solution method was based on Ritz method and Chebyshev polynomials. According to the results, the frequency variation depends on the volume fraction of carbon nano-tubes. Shams and Soltani (2016) have investigated the buckling response of composite plates that are reinforced with CNT on elastic foundation. In this study the CNTs are distributed uniformly through the thickness of plate. According to this study, the parameters such as geometric and mechanical properties have significant effect on buckling behavior of laminated CNTRC plates.

Selim *et al.* (2017) utilized an element-free method based on Reddy's higher-order shear deformation theory to study active vibration control of carbon nano-tube reinforced composite plates with piezoelectric layers. In this study, the effects of CNTs volume fraction, CNTs distribution through thickness and piezoelectric layer thickness on the natural frequency were considered.

Shen (2012) studied thermal buckling of nanocomposite cylindrical shells reinforced by single-walled nano-tubes (SWNT). In this study two different distributions of CNTs through thickness namely uniform distributed (UD) and functionally graded (FG) reinforcements were considered. The results indicated that the buckling temperature and thermal postbuckling strength of carbon nano-tube reinforced composite cylindrical shell are increased due to the existence of CNTs.

Wang and Shen (2012, 2011) have investigated the large amplitude vibration and nonlinear bending of CNTRC plate on elastic foundation in thermal environments. In this study, the effects of nano-tube volume fraction, temperature variation, foundation parameters and boundary conditions on nonlinear vibration and bending response of sandwich plates reinforced with CNTs were studied.

Rafiee *et al.* (2014) investigated the nonlinear dynamic stability of piezoelectric functionally graded CNTRC plates subjected to thermal and electrical loadings. They employed the classical plate theory and von Karman geometric nonlinearity assumptions to obtain the governing equations of the system.

Ribeiro (2016) investigated the nonlinear vibration modes of CNTs were actuated by electrostatic forces. The harmonic balance and arc-length continuation methods were utilized to solve the problem. In this study, the non-local effects were combined with geometrical nonlinearity. Based on the results, these parameters can affect the natural frequencies and degrees of softening or hardening behaviors.

Benedict and Roy (2016) utilized finite element method to study vibration of functionally graded carbon nano-tube reinforced composite (FG-CNTRC) shell structures. In

*Corresponding author, Ph.D.
E-mail: aliaminyazdi@qiet.ac.ir

order to study the effects of CNTs on the damping capacity of shell structures they used Rayleigh damping model.

Fazelzadeh *et al.* (2015) investigated the effect of CNTs on aeroelastic nonlinear behavior of composite plates subjected to supersonic flow. A parametric investigation has been carried out to study the effect of volume fraction, geometrical parameters and inplane forces on flutter pressure of nanocomposite plates.

Guo and Zhang (2016) have considered the effects of the forcing excitations on periodic and chaotic motions of reinforcement CNT composite plate. Wang *et al.* (2016) employed multi-Kantorovich Galerkin method to study buckling and free vibration of thin carbon nano-tube reinforced composite plates. In this study the accuracy of the presented method was evaluated for different boundary conditions.

Ke *et al.* (2010) studied the nonlinear free vibration of functionally graded reinforced nanocomposite beams. In this study the Timoshenko beam theory and von Karman geometric nonlinearity were considered. According to the results of this study, CNT volume fraction increasing yields frequency growth of FG-CNTRC beams. Additionally, the effects of symmetrical distribution of CNTs on frequency variation are more effective than unsymmetrical distributions.

Zhang *et al.* (2014) used mesh-free kp-Ritz method to study the large deflection geometrically nonlinear behavior of FG-CNT cylindrical panels subjected to mechanical loads. In this study the effects of different parameters including span angle, thickness, volume fraction of CNTs and boundary conditions on nonlinear behavior of panels were investigated.

Kiani (2017) used first shear deformation shell theory with Sanders kinematics to study the vibration behavior of spherical panels reinforced by CNTs. According to this study the functionally graded pattern with more CNTs in polymer matrix is more effective on variation of frequencies. Selim *et al.* (2017) studied the impact effect on CNTRC plates. They employed the finite element method and Reddy's higher order shear deformation theory to analyze the impact of CNTRC plates.

Ardastani *et al.* (2017) tried to find the optimal fiber orientation to improve the bending and vibration behavior of reinforced skew composite plate. Based on the results of this study, the correct chosen of the fiber orientation plays significant role in static and vibration behavior of reinforced composite plates. Kiani (2016) studied free vibration of composite skew plates reinforced by CNTs. The first shear deformation theory and Ritz method were utilized to predict the natural frequencies of skew plate. As it was mentioned in this study, the CNTs volume fraction and their distribution along the plate thickness can affect the plate natural frequencies, significantly. Additionally, Mirzaei and Kiani (2016) investigated free vibration of cylindrical composite panels reinforced by CNTs. Zhang *et al.* (2017) studied the behavior of functionally graded CNTs reinforced cylindrical shells under effect of impact. A linearized contact law was employed to find a contact coefficient to simulate the effect of contact load. Effect of piezoelectric layers on free vibration of CNTs reinforced

composite plates were studied by Kian (2016). Based on the results of this investigation, closed circuit plate has higher natural frequency in comparison with open circuit plate.

Ansari and Gholami (2016) used higher order deformable theory to investigate the nonlinear behavior vibration response of composite plates reinforced by CNTs under harmonic excitation. In this study the effect of different edge support and CNTs volume fraction on frequency and force response curves were studied. In another study Gholami and Ansari (2018) developed weak form of functionally graded graphene platelet (GPL) reinforced composite plate. In this study the effect different parameters including GPL weight fraction, distribution of GPL pattern and their geometry on geometrically nonlinear harmonically excited vibration composite plate reinforced by functionally graded graphene platelet. Additionally, Gholami and Ansari (2017) investigation regarded the effect of large deflection on nonlinear vibration of composite plate reinforced by functionally graded graphene platelet.

Ansari *et al.* (2014) and Gholami *et al.* (2017) investigated nonlinear forced vibration of Timoshenko beams and imperfect higher-order shear deformable composite beams reinforced by CNTs, respectively.

Ansari and his co-authors presented a numerical solution for forced vibration of the functionally graded CNTs composite plates (2015) and analytical one to investigate the effect of piezoelectric layers on postbuckling of functionally graded CNTs reinforced composite shells (2016).

Ghorbanpour Arani *et al.* (2017) studied vibration of moving functionally graded CNTs reinforced composite plate. In this study the effect of different shear deformation theory, moving speed, CNTs volume fraction and distribution were investigated. According to the results, axially moving speed plays a significant role in predicting the natural frequency of the reinforced composite plates. Additionally, Ghorbanpour and his co-authors (2016) investigated vibration of axially moving multiscale nanocomposite plate. To investigate the effects of damping coefficient, shear modulus and orthotropy angle an orthotropic visco Pasternak foundation model was developed.

Ghorbanpour and Haghparast (2017) used higher order shear deformation theory to investigate instability of moving reinforced composite plates by CNTs under the effect of initial tension. According to the results, appending CNTs to composite plate yields the growth of plate critical moving speed.

As the knowledge of the author, the amount of investigations regarding free vibration and buckling of CNTRC plates have been increased recently but few studies conducted to analysis the forced vibration and active control of these plates. The main aim of this study is to investigate the nonlinear forced vibration of carbon nano-tube reinforcement composite plates on nonlinear elastic foundations. It is assumed that the plate is bonded with piezoelectric layers on top and bottom surface of plate. The characteristic equation of the system is obtained using the classical plate theory with von Karman geometric nonlinearity. It is assumed that carbon nano-tubes are

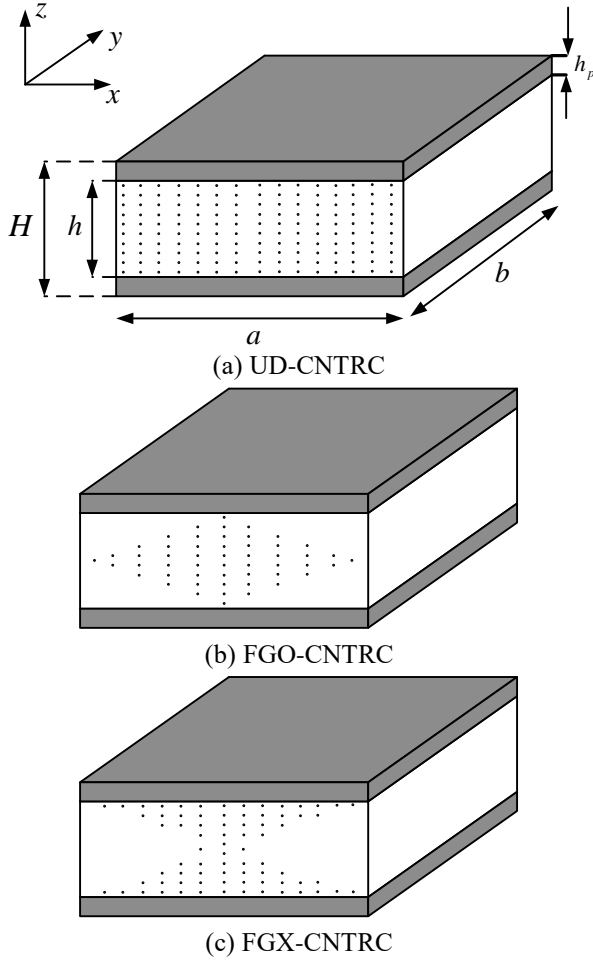(a) UD-CNTRC

(b) FGO-CNTRC

(c) FGX-CNTRC

Fig. 1 Distribution of carbon nanotubes along thickness direction for reinforced piezoelectric composite plate

distributed along thickness in two different manner namely uniformly distribution (UD) and functionally graded (FG). The homotopy perturbation method (HPM) is utilized to study the large amplitudes effect on nonlinear response of excited CNTRC plates. In this study the effect of parameters such as elastic foundation parameters, large amplitudes, carbon nano-tube volume fractions and piezoelectric applied voltage are discussed in details.

2. Description of mathematical model

A rectangular carbon nano-tube-reinforced composite (CNTRC) plate with length a, width b and thickness H is considered in Fig. 1. The three different symmetric carbon nano-tube reinforcement distributions through the thickness are shown. The top and bottom of the CNTRC plate are bonded with piezoelectric layers perfectly. The rule of mixture is employed to obtain the Young and shear modulus of CNTRC plate. It is assumed that the CNTRC is combination of an isotropic matrix with single walled carbon nano-tube (SWCNT). According to this it can be written (Shen 2012)

$$E_{11} = \eta_1 V_{CN} E_{11}^{CN} + V_m E^m \tag{1}$$

$$\frac{\eta_2}{E_{22}} = \frac{V_{CN}}{E_{22}^{CN}} + \frac{V_m}{E^m} \tag{2}$$

$$\frac{\eta_3}{G_{12}} = \frac{V_{CN}}{G_{12}^{CN}} + \frac{V_m}{G^m} \tag{3}$$

where E^m, G^m refer to the Young modulus and shear modulus of isotropic host and E_{ij}, G_{ij} are the material properties of SWCNT. Parameters $\eta_i, (i = 1,2,3)$ are introduced to consider the scale dependent material properties of CNT. The volume fractions of carbon nano-tube and matrix are related to each other as follows

$$V_{CN} + V_m = 1 \tag{4}$$

V_{CN} for different distributions of carbon nano-tube along thickness direction can be considered as (Shen 2012)

$$\begin{aligned} \text{UD:} & & V_{CN}^* \\ \text{FG-X:} & & \left(2 - \frac{4|z|}{h}\right) V_{CN}^* \\ \text{FG-O:} & & \left(\frac{4|z|}{h}\right) V_{CN}^* \end{aligned} \tag{5}$$

$$V_{CN}^* = \frac{\omega_{CN}}{\omega_{CN} + (\rho^{CN}/\rho^m) - (\rho^{CN}/\rho^m)\omega_{CN}} \tag{6}$$

where ρ^{CN} and ρ^m are mass densities for carbon nano-tubes and matrix respectively and ω_{CN} is the mass fraction of the SWCNTs. Additionally, the Poisson's ratio and mass density for CNTRC plate can be written as follows

$$\nu_{12} = V_{CN}^* \nu_{12}^{CN} + V_m \nu^m \tag{7}$$

$$\rho = V_{CN} \rho^{CN} + V_m \rho^m \tag{8}$$

where ν_{12}^{CN} and ν^m are the Poisson ratio of CNTs and matrix, respectively. Using the von Karman deformation assumptions, the strain displacement relations are as follows

$$\{\varepsilon_{ij}\} = \{\varepsilon_{ij}^0\} + z\{\kappa_{ij}\}$$

$$\begin{Bmatrix} \varepsilon_{xx}^0 \\ \varepsilon_{yy}^0 \\ \varepsilon_{xy}^0 \end{Bmatrix} = \begin{Bmatrix} \dfrac{\partial u}{\partial x} + \dfrac{1}{2}\left(\dfrac{\partial w}{\partial x}\right)^2 \\[2mm] \dfrac{\partial v}{\partial y} + \dfrac{1}{2}\left(\dfrac{\partial w}{\partial y}\right)^2 \\[2mm] \dfrac{1}{2}\left(\dfrac{\partial u}{\partial y} + \dfrac{\partial v}{\partial x} + \dfrac{\partial w}{\partial x}\dfrac{\partial w}{\partial y}\right) \end{Bmatrix} \begin{Bmatrix} \kappa_{xx} \\ \kappa_{yy} \\ \kappa_{xy} \end{Bmatrix}$$

$$= -\begin{Bmatrix} \dfrac{\partial^2 w}{\partial x^2} \\[2mm] \dfrac{\partial^2 w}{\partial y^2} \\[2mm] 2\dfrac{\partial^2 w}{\partial x \partial y} \end{Bmatrix} \tag{9}$$

Using the classical plate theory assumptions, the constitutive equations for a layer can be written as follows (Selim *et al.* 2017)

$$\begin{Bmatrix} \sigma_x \\ \sigma_y \\ \sigma_{xy} \end{Bmatrix} = \begin{bmatrix} Q_{11} & Q_{12} & 0 \\ Q_{12} & Q_{22} & 0 \\ 0 & 0 & Q_{66} \end{bmatrix} \begin{Bmatrix} \varepsilon_x \\ \varepsilon_y \\ \varepsilon_{xy} \end{Bmatrix} - \begin{Bmatrix} e_{31} E_z \\ e_{32} E_z \\ 0 \end{Bmatrix}$$

$$\begin{Bmatrix} D_x \\ D_y \\ D_z \end{Bmatrix} = \begin{Bmatrix} 0 \\ 0 \\ e_{31}\varepsilon_x + e_{32}\varepsilon_y \end{Bmatrix} + \begin{bmatrix} \epsilon_{11} & 0 & 0 \\ 0 & \epsilon_{22} & 0 \\ 0 & 0 & \epsilon_{33} \end{bmatrix} \begin{Bmatrix} 0 \\ 0 \\ E_z \end{Bmatrix} \tag{10}$$

where $\{\sigma\}$ is the stress vector, $[Q]$ is stress reduced stiffness matrix, $\{\varepsilon\}$ is the strain vector, $[e]$ is the piezoelectric matrix, $\{E\}$ is the electrical field vector, $\{D\}$ is the electrical displacement vector and $[\epsilon]$ is the permittivity matrix. The electric field vector can be expressed as follows (Selim *et al.* 2017)

$$E = -grad\ \phi \tag{11}$$

where ϕ is the electrical potential vector. The Q_{ij} stiffness coefficients can be expressed as follows (Wang 2012)

$$
\begin{aligned}
Q_{11} &= \frac{E_{11}}{1-v_{12}v_{21}} \\
Q_{12} &= \frac{v_{12}E_{22}}{1-v_{12}v_{21}} \\
Q_{22} &= \frac{E_{22}}{1-v_{12}v_{21}} \\
Q_{66} &= G_{12}
\end{aligned}
\tag{12}
$$

For CNTRC host and

$$
\begin{aligned}
Q_{11p} = Q_{22p} &= \frac{E_p}{1-v_p^2} \\
Q_{12p} &= \frac{v_p E_p}{1-v_p^2} \\
Q_{66p} &= \frac{E_p}{2(1+v_p)}
\end{aligned}
\tag{13}
$$

for the piezoelectric layers. To derive the governing equation of the system for the symmetric cross-ply laminated plate the Hamilton's principle is employed

$$\delta \int_{t_0}^{t_1} (T - U - W_e)\ dt = 0 \tag{14}$$

where

$$U = \frac{1}{2}\int_V (\sigma^T \varepsilon - D^T E)dV \tag{15}$$

$$U = \frac{1}{2}\int_0^a \int_0^b \left\{ \begin{array}{c} \{\varepsilon_0\}^T[A]\{\varepsilon_0\} + \{\kappa\}^T[D]\{\kappa\} \\ -\{\varepsilon_0\}^T[e]^T\{E\} - \{E\}^T[\epsilon]^T\{E\} + K_1 w^2 + K_2 w^4 \\ -(Gw_x)_{,x} - (a/b)^2 (Gw_y)_{,y} \end{array} \right\} dx\, dy \tag{16}$$

$$T = \frac{1}{2}\int_0^a \int_0^b \left\{ I_0 - I_2 \left[\frac{\partial^2 w}{\partial x^2} + \frac{\partial^2 w}{\partial y^2} \right] \right\} \left(\frac{\partial w}{\partial t} \right)^2 dx\, dy \tag{17}$$

$$W_e = \int_0^a \int_0^b \left\{ I_0 \xi w \frac{\partial w}{\partial t} - \phi\, q(t) - f\, w \right\} dx\, dy \tag{18}$$

$$I_0, I_2 = \int_{-H/2}^{H/2} \rho(z)\,(1, z^2)dz \tag{19}$$

Where U is the strain energy of the plate, T is the kinetic energy of the plate, W_e is the work done by external forces, I_0 and I_2 are the mass moments inertia, f is the external mechanical load, K_1, K_2 are the linear and nonlinear elastic foundations coefficients, G is the shear parameter of the Pasternak foundation model, ξ is damping ratio, q is the external surface charge. Substituting Eqs. (16) through (18) into Eq. (14) yields to a set of partial differential equations as follows

$$\frac{\partial N_x}{\partial x} + \frac{\partial N_{xy}}{\partial y} = I_0 \frac{\partial^2 u}{\partial t^2} \tag{20a}$$

$$\frac{\partial N_y}{\partial y} + \frac{\partial N_{xy}}{\partial x} = I_0 \frac{\partial^2 v}{\partial t^2} \tag{20b}$$

$$
\begin{aligned}
&\frac{\partial^2 M_x}{\partial x^2} + \frac{\partial^2 M_{xy}}{\partial x \partial y} + \frac{\partial^2 M_y}{\partial y^2} + \frac{\partial}{\partial x}\left(N_x \frac{\partial w}{\partial x} \right) \\
&\quad + \frac{\partial}{\partial y}\left(N_y \frac{\partial w}{\partial y} \right) + \frac{\partial}{\partial x}\left(N_{xy} \frac{\partial w}{\partial y} \right) \\
&\quad + \frac{\partial}{\partial y}\left(N_{xy} \frac{\partial w}{\partial x} \right) - K_L w - K_{NL} w^3 \\
&\quad + G\left(\frac{\partial^2 w}{\partial x^2} + \left(\frac{a}{b}\right)^2 \frac{\partial^2 w}{\partial y^2} \right) \\
&\quad + f(x, y, t) \\
&= I_0 \frac{\partial^2 w}{\partial t^2} + 2\xi I_0 \frac{\partial w}{\partial t} \\
&\quad - I_2 \frac{\partial^2}{\partial t^2}\left(\frac{\partial^2 w}{\partial x^2} + \frac{\partial^2 w}{\partial y^2} \right)
\end{aligned}
\tag{20c}
$$

The variations in resultant forces and moments are

$$
\begin{Bmatrix} N_{xx} \\ N_{yy} \\ N_{xy} \end{Bmatrix} = \begin{bmatrix} A_{11} & A_{12} & 0 \\ A_{12} & A_{22} & 0 \\ 0 & 0 & A_{66} \end{bmatrix} \begin{Bmatrix} \varepsilon_{xx}^0 \\ \varepsilon_{yy}^0 \\ \gamma_{xy}^0 \end{Bmatrix} + - \begin{Bmatrix} N_{xx}^P \\ N_{yy}^P \\ N_{xy}^P \end{Bmatrix} \tag{21}
$$

$$
\begin{Bmatrix} M_{xx} \\ M_{yy} \\ M_{xy} \end{Bmatrix} = \begin{bmatrix} D_{11} & D_{12} & 0 \\ D_{12} & D_{22} & 0 \\ 0 & 0 & D_{66} \end{bmatrix} \begin{Bmatrix} \kappa_{xx} \\ \kappa_{yy} \\ \kappa_{xy} \end{Bmatrix} - \begin{Bmatrix} M_{xx}^P \\ M_{yy}^P \\ M_{xy}^P \end{Bmatrix} \tag{22}
$$

where

$$
\begin{aligned}
(A_{ij}, B_{ij}, D_{ij}) &= \int_{-H/2}^{-h/2} Q_{ij}^p (1, z, z^2)dz \\
&\quad + \int_{-h/2}^{h/2} Q_{ij}(1, z, z^2)dz \\
&\quad + \int_{h/2}^{H/2} Q_{ij}^p (1, z, z^2)dz, \\
i &= 1, 2, 6
\end{aligned}
\tag{23}
$$

$$
\begin{Bmatrix} N_{xx}^P \\ N_{yy}^P \\ N_{xy}^P \end{Bmatrix} = 2\int_{h/2}^{H/2} \begin{Bmatrix} e_{31} \\ e_{32} \\ 0 \end{Bmatrix} E_z\, dz, \tag{24}
$$

$$
\begin{Bmatrix} M_{xx}^P \\ M_{yy}^P \\ M_{xy}^P \end{Bmatrix} = 2\int_{h/2}^{H/2} \begin{Bmatrix} e_{31} \\ e_{32} \\ 0 \end{Bmatrix} E_z\, z\, dz \tag{25}
$$

It should be noted that for symmetric configuration the strength-bending coupling stiffness will not be appeared. To investigate this problem the following boundary conditions are considered

$$for\ x = 0, a\ \ \ v = w = 0$$

$$for\ y = 0, b\ \ \ u = w = 0$$

The following allowable functions can satisfy the boundary condition

$$u = U(t) \cos\frac{m\pi x}{a} \sin\frac{n\pi y}{b}$$
$$v = V(t) \sin\frac{m\pi x}{a} \cos\frac{n\pi y}{b} \qquad (26)$$
$$w = W(t) \sin\frac{m\pi x}{a} \sin\frac{n\pi y}{b}$$

In this study, it is assumed that the piezoelectric panel is thin and the electric potential is distributed through the thickness linearly. In this case, only the electric field along thickness directions none zero and can be considered as (Selim *et al.* 2017)

$$E_z = \frac{V(t)}{h_p} \qquad (27)$$

Substituting Eq. (26) into Eqs. (20) and applying Galerkin method, the $U(t)$ and $V(t)$ can be written in terms of $W(t)$ from the first two equations and substituting in the third one yields

$$L_1 \frac{d^2 W(t)}{dt^2} + 2I_0\xi \frac{dW(t)}{dt} + L_2 W(t) + L_3 W^3(t) = Q \sin\Omega t \qquad (28)$$

where

$$L_1 = I_0 + I_2 \left[\left(\frac{m\pi}{a}\right)^2 + \left(\frac{n\pi}{b}\right)^2\right] \qquad (29a)$$

$$L_2 = T_6 \qquad (29b)$$

$$L_3 = T_7 + 2(2T_1T_3T_5 - T_2T_5^2 - T_4T_3^2)/(T_2T_4 - T_1^2) \quad (29c)$$

where Ω is the excited frequency and the T_i coefficients that are functions of the geometric and mechanical properties of the plate which are defined in Appendix. To solve Eq. (28) the following initial conditions are considered

$$W(0) = W_{max}, \quad \frac{dW(0)}{dt} = 0 \qquad (30)$$

$$\omega_0^2 = L_2/L_1 \qquad (31)$$

The homotopy perturbation method (HPM) is used to study the effect of large amplitudes on the nonlinear response of CNTRC plate. According to this method, the following homotopy is constructed (He 1999)

$$L_1\ddot{W}(t) + L_2 W(t) = p[Q \sin\Omega t - 2I_0\xi\dot{W}(t) - L_3 W^3(t)] \qquad p \in [0,1] \qquad (32)$$

where p is an embedding parameter. The solution of Eq. (32) can be expressed as a series of power p

$$W = W_0 + pW_1 + p^2 W_2 + \cdots \qquad (33)$$

Based on the concept of perturbation method the excited frequency can be expanded by embedding parameter and natural frequency ω_0

$$\Omega^2 = \omega_0^2(1 + p\sigma_1 + p^2\sigma_2 + \cdots) \qquad (34)$$

where σ is the detuning parameter. Introducing the new variable $\tau = \Omega t$, the Eq. (32) can re-written as follows

$$L_1\Omega^2\ddot{W}(\tau) + L_2 W(\tau) = p[Q \sin\tau - 2I_0\xi\Omega\dot{W}(\tau) - L_3 W^3(\tau)] \qquad p \in [0,1] \qquad (35)$$

Substituting Eqs. (33) and (34) into Eq. (35) and equating the terms with identical power of p, one can obtained

$$\ddot{W}_0 + W_0 = 0 \qquad (36)$$

$$\ddot{W}_1 + W_1 = \frac{Q}{L_1\omega_0^2}\sin\tau - \frac{2I_0\xi}{L_1\omega_0^2}\Omega\dot{W}_0 - \frac{L_3}{L_1\omega_0^2}W_0^3 - \sigma_1\ddot{W}_0 \qquad (37)$$

The solution of Eq. (36) can be followed as

$$W_0 = W_m \cos(\tau + \theta) \qquad (38)$$

where θ is the phase angle. Using Eq. (38) and substituting into Eq. (37) one can obtain

$$\ddot{W}_1 + W_1 = \frac{Q}{L_1\omega_0^2}\sin\tau - \frac{2I_0\xi}{L_1\omega_0^2}\Omega\ W_{max}\sin(\tau + \theta)$$
$$+ \left(\sigma_1 W_{max} - \frac{3}{4}\frac{L_3 W_{max}^3}{L_1\omega_0^2}\right)\cos(\tau + \theta) - \frac{1}{4}\frac{L_3 W_{max}^3}{L_1\omega_0^2}\cos 3(\tau + \theta) \qquad (39)$$

Solving Eq. (39) can be written

$$W_1 = \frac{1}{2}\left[\frac{2I_0\xi}{L_1\omega_0^2}\Omega\ W_{max}\sin\theta + \left(\sigma_1 W_{max} - \frac{3}{4}\frac{L_3 W_{max}^3}{L_1\omega_0^2}\right)\cos\theta\right]\sin\tau$$
$$- \frac{1}{2}\left[\frac{2I_0\xi}{L_1\omega_0^2}\Omega\ W_{max}\cos\theta + \left(\frac{3}{4}\frac{L_3 W_{max}^3}{L_1\omega_0^2} - \sigma_1 W_{max}\right)\sin\theta + \frac{Q}{L_1\omega_0^2}\right]\cos\tau$$
$$+ \frac{L_3 W_{max}^3}{32 L_1\omega_0^2}\cos 3(\tau + \theta) \qquad (40)$$

To stabilize the nonlinear response the secular terms should be eliminated. In this case, the coefficients of $\cos\tau$ and $\sin\tau$ must be zero. According to this fact and eliminating the parameter θ one can obtain

$$\left(\frac{2I_0\xi}{L_1\omega_0^2}\Omega\right)^2 + \left(\sigma_1 - \frac{3}{4}\frac{L_3 W_{max}^2}{L_1\omega_0^2}\right)^2 = \left(\frac{Q}{W_{max}L_1\omega_0^2}\right)^2 \quad (41)$$

The frequency response equation in terms of detuning parameter can be written as follows

$$\sigma_1 = \mp\sqrt{\left(\frac{Q}{W_{max}L_1\omega_0^2}\right)^2 - \left(\frac{2I_0\xi}{L_1\omega_0^2}\Omega\right)^2} + \frac{3}{4}\frac{L_3 W_{max}^2}{L_1\omega_0^2} \quad (42)$$

For the first-order approximation of $W(\tau)$, we have

Table 1 CNT efficiency parameters for different values of V_{CN}^* (Shen 2012)

V_{CN}^*	η_1	η_2	η_3
0.12	0.137	1.022	0.715
0.17	0.142	1.626	1.138
0.28	0.141	1.585	1.109

Table 2 Comparison the dimensionless fundamental natural frequency $\left(\Omega = \omega(a^2/h)\sqrt{\rho^m/E_m}\right)$ of CNTRC plate of the presented study with data available in the literature ($a/h = 100, K_L = K_{NL} = 0$)

Distribution	h_p/H	V_{CN}^*					
		0.12		0.17		0.28	
		This study	Ref. (Rafiee *et al.* 2014)	This study	Ref. (Rafiee *et al.* 2014)	This study	Ref. (Rafiee *et al.* 2014)
UD CNTRC	0	19.006	18.059	22.875	21.806	28.268	27.077
	0.1	21.574	20.512	23.035	22.043	25.484	24.504
	0.2	23.716	22.747	24.587	23.641	26.196	25.14
FGO CNTRC	0	13.844	13.376	16.757	16.144	20.499	19.711
	0.1	19.674	18.881	20.558	19.787	22.012	21.145
	0.2	22.633	21.825	23.352	22.326	24.021	23.097

Table 3 Comparison the non-dimensional natural frequency $\left(\Omega = \omega(a^2/h)\sqrt{\rho^m/E_m}\right)$ and frequency ratios for CNTRC square plates ($a/h = 100, K_L = K_{NL} = 0$) with different vibration amplitudes

		Ω	W_{max}/h				
			0.2	0.4	0.6	0.8	1
UD	This study	22.3933	1.0734	1.1647	1.3119	1.4748	1.6795
	Ref. (Wang 2012)	21.6989	1.0322	1.1232	1.2603	1.4304	1.6231
FG-X	This study	11.3318	1.1724	1.4838	1.8961	2.363	2.8348
	Ref. (Wang 2012)	10.9065	1.122	1.4268	1.8249	2.2678	2.7337

Table 4 Comparison of first five natural frequencies of square Ti-6AL-4V plate with piezoelectric layers ($a/b = 1, a/h = 80$)

| Natural Frequencies	This Study	Ref. (Kiani 2016)
Ω_1	147.71	145.35
Ω_2	366.13	363.05
Ω_3	367.02	363.05
Ω_4	727.11	725
Ω_5	728.04	725

$$\sigma_1 = \left(\frac{\Omega}{\omega_0}\right)^2 - 1 \qquad (43)$$

Substituting Eq. (43) into Eq. (42), results in

$$\left[\frac{2I_0\xi}{L_1\omega_0}\left(\frac{\Omega}{\omega_0}\right)\right]^2 + \left[1 - \left(\frac{\Omega}{\omega_0}\right)^2 + \frac{3}{4}\frac{L_3 W_m^2}{L_1\omega_0^2}\right]^2 = \left(\frac{Q}{W_m L_1 \omega_0^2}\right)^2 \qquad (44)$$

Table 5 Comparison of non-linear to linear frequency ratio for thin cross-ply laminated plates

W_{max}/h	(0/90)$_s$, a/b=1, a/h=50		(0/90)$_2$, a/b=2, a/h=50	
	Ref. (Singh *et al.* 1990)	Present study	Ref. (Singh *et al.* 1990)	Present study
0.25	1.0535	1.0547	1.0645	1.0679
0.5	1.2038	1.2167	1.2427	1.2563
0.75	1.4172	1.432	1.4905	1.4221
1	1.6691	1.7119	1.7787	1.7818
1.5	2.2355	2.2825	2.4178	2.4768
2	2.8439	2.9129	3.0976	3.1332
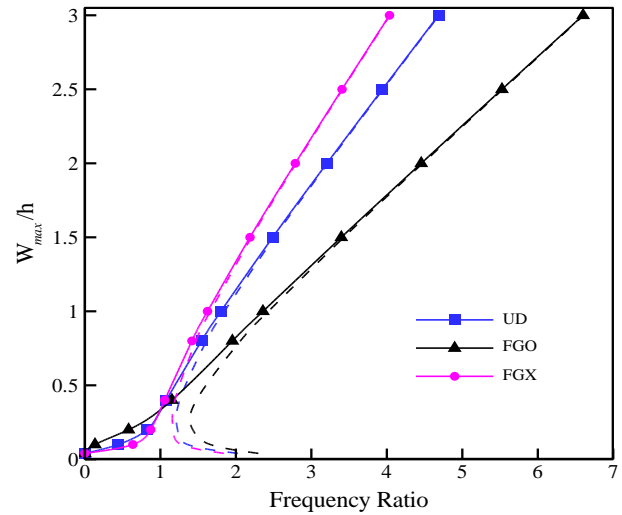
Fig. 2 Variation of frequency ratio versus W_{max}/h for different configuration of CNTRC plate, ($T = 300, h_p = 0$, $\xi = 0.1$, $a/b = 1, K_L = K_{NL} = 0, V_{CN}^* = 0.28, V_0 = 0, Q \neq 0, a/h = 50$)

In the next section a detailed parametric studies are presented to demonstrate the nonlinear response of CNTRC plates.

3. Numerical results and discussions

The Poly (methyl methacrylate), referred to as PMMA, is selected for the matrix and its properties are assumed to be $\rho^m = 1150\ kg/m^3$, $v^m = 0.34$ and $E^m = (3.52 - 0.0034\ T)GPa$ where $T = T_0 + \Delta T$ and T_0 is the room temperature. The piezoelectric material properties are $E_p = 63\ GPa$, $\rho_p = 7600\ kg/m^3$, $v_p = 0.3$ and $e_{31} = e_{32} = 17.6\ C/m^2$. In Table 1, the CNT efficiency parameters $\eta_i\ (i = 1,2,3)$ are estimated according by matching the mechanical properties of CNTRC obtained by means of MD simulation with those extended from the rules of mixture are given. In all cases, in this study the linear and non-linear dimensional Winkler elastic foundation parameters are defined as follows

$$(K_L)_{ND} = \frac{K_L a^4}{D_{11}} \qquad (45)$$

$$(K_{NL})_{ND} = \frac{K_{NL} a^4}{A_{11}} \qquad (46)$$

$$G_{ND} = \frac{Ga^2}{D_{11}} \qquad (47)$$

In Tables 2 through 5, the non-dimensional natural frequency and frequency ratio at different vibration amplitudes of a square CNTRC plate is given. The predicted results are compared with data which are available in literature. The results have shown the level of confidence that can be expected from the presented method.

Fig. 2 demonstrates the effect of CNT distribution through thickness on frequency ratio for three different types of CNTRC plates. According to the results, among these different existing types, by increasing the vibration amplitudes, the FGO configuration with maximum value of CNT at the midplane, has greater frequency ratio in comparison with two other types of CNTRC plates.

In Fig. 3, the free ($Q = 0$) and forced ($Q \neq 0$) harmonic response of CNTRC plate around its first mode of vibration for two different types of CNTRC namely FGO and UD are shown. As common behavior response in nonlinear vibratory systems, the free response points give rise to jump phenomena. Additionally, it is shown, the degree of hardening for these two types of CNTRC plate is different. At large amplitude vibrations the FGO plates intensify the hardening degree.
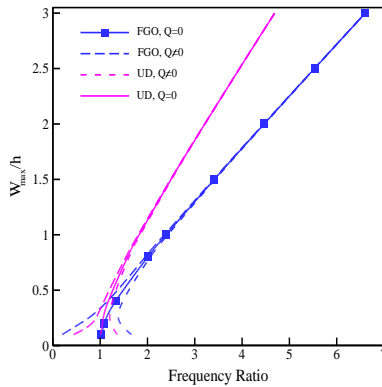

Fig. 3 Free and forced response versus W_{max}/h for CNTRC plate, $(T = 300, h_p = 0, \xi = 0, a/b = 1, K_L = K_{NL} = 0, V_0 = 0, a/h = 50)$
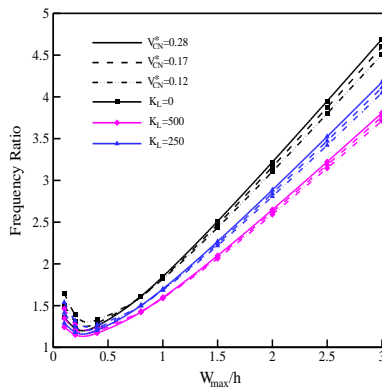

Fig. 4 Effect of linear elastic foundation parameter on frequency ratio versus W_{max}/h for Uni-directional CNTRC plate, $(T = 300, h_p = 0, \xi = 0, a/b = 1, K_{NL} = 0, V_0 = 0, Q \neq 0, a/h = 100)$
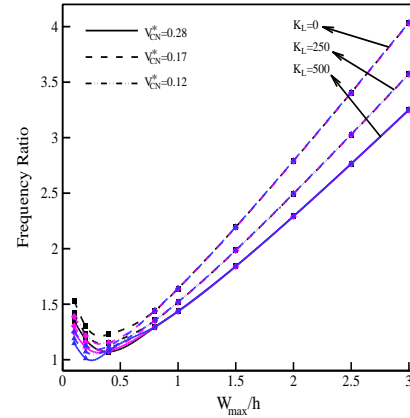

Fig. 5 Effect of linear elastic foundation parameter on frequency ratio versus W_{max}/h for FGX CNTRC plate, $(T = 300, h_p = 0, \xi = 0.1, a/b = 1, K_{NL} = 0, V_0 = 0, Q \neq 0, a/h = 100)$
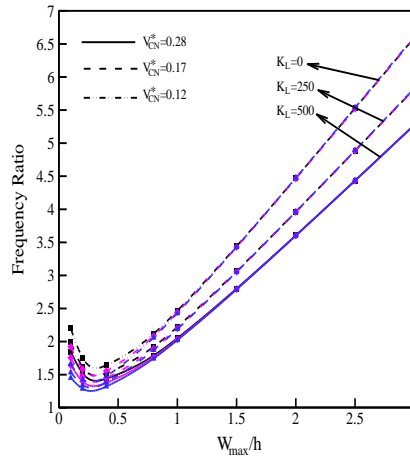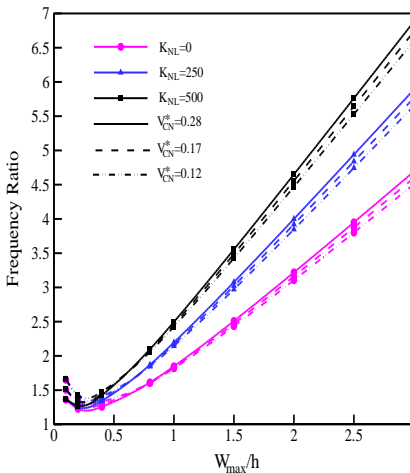

Fig. 6 Effect of linear elastic foundation parameter on frequency ratio versus W_{max}/h for FGO CNTRC plate, $(T = 300, h_p = 0, \xi = 0.1, a/b = 1, K_{NL} = 0, V_0 = 0, Q \neq 0, a/h = 100)$

Fig. 7 Effect of Non-linear elastic foundation parameter on frequency ratio versus W_{max}/h for Uni-directional CNTRC plate, $(T = 300, h_p = 0, \xi = 0, a/b = 1, K_L = 0, V_0 = 0, Q \neq 0, a/h = 100)$
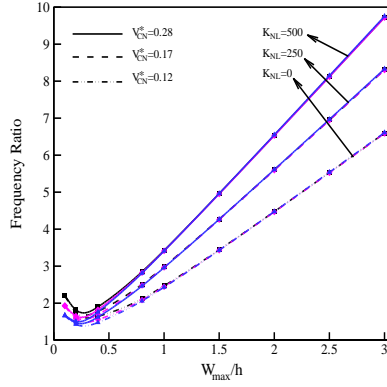
Fig. 8 Effect of Non-linear elastic foundation parameter on frequency ratio versus W_{max}/h for FGO CNTRC plate, $T = 300, h_p = 0, \xi = 0, a/b = 1, K_L = 0, V_0 = 0, Q \neq 0$

Fig. 11 Effect of applying voltage on free vibration response of FGO CNTRC plate, $\left(T = 300, \xi = 0, a/b = 1, K_L = K_{NL} = 0, Q = 0, h_p/H = 0.2, a/h = 100\right)$
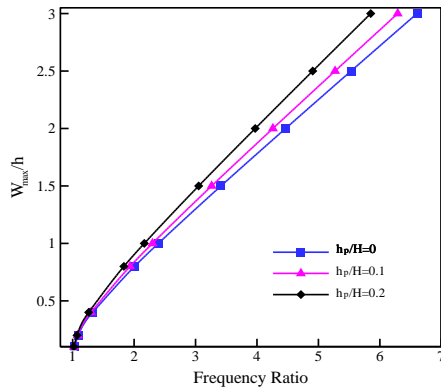

Fig. 9 Effect of piezoelectric layer thickness on free vibration response of FGO CNTRC plate, $(T = 300, \xi = 0, a/b = 1, K_L = K_{NL} = 0, V_0 = 0, Q = 0, a/h = 100)$

Fig. 12 Variation of W_{max}/h with excitation force amplitude for different value of detuning parameters
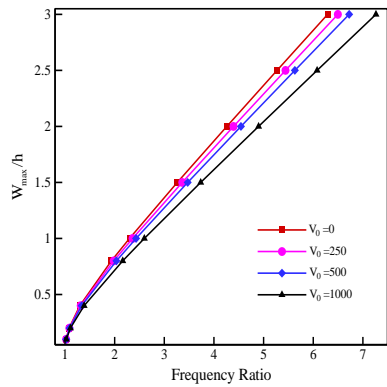

Fig. 10 Effect of applying voltage on free vibration response of FGO CNTRC plate, $\left(T = 300, \xi = 0, a/b = 1, K_L = K_{NL} = 0, Q = 0, h_p/H = 0.1, a/h = 100\right)$

Fig. 13 Effect of linear elastic foundation parameter on nonlinear response of CNTRC plate

In Figs. 4 through 6, the effect of linear elastic foundation parameter and CNT volume fractions on frequency ratio are shown. Based on the results, for all three different types of CNTRC plates for $W_{max}/h < 1$, increasing the CNT volume fraction results decreasing of frequency ratio. On the other hand, for $W_{max}/h>1$ variation of CNT volume fraction of functionally graded CNTRC plate has no effect on frequency ratio while for unidirectional plate increasing the volume fraction yields
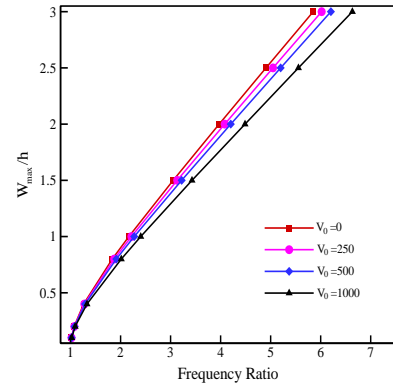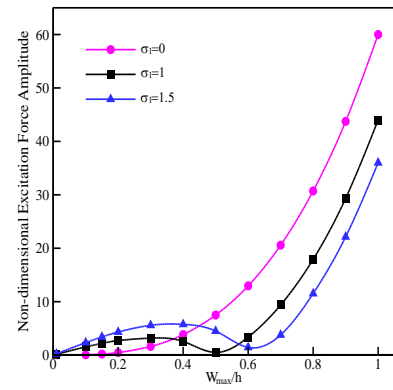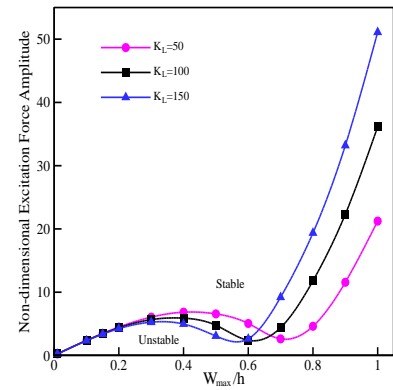
increasing of frequency ratio. Additionally, it should be noted that the growth of linear elastic foundation parameter yields decreasing of frequency ratio of CNTRC plates. On the other word, the increasing of linear elastic foundation can reduce the hardening degree of CNTRC plates.

In Figs. 7 and 8, the results for similar investigation for nonlinear elastic foundation parameter on frequency ratio for CNTRC plates are illustrated. For $W_{max}/h < 1$, the variation of CNT volume fraction has significant effect on discrepancy of frequency ratio, while for $W_{max}/h>1$ the variation of CNT volume fraction is not capable to affect
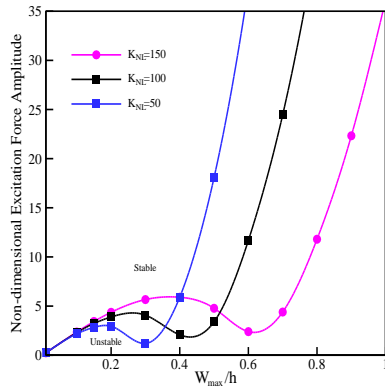
Fig. 14 Variation of Nonlinear response of CNTRC plate with nonlinear elastic foundation parameter

Table 6 Effect of applied voltage on frequency ratio of FGO CNTRC plate for different piezoelectric thickness ($T = 300, \ \xi = 0, a/b = 1, K_L = K_{NL} = 0, Q = 0, a/h = 100$)

W_m/H	$V_0 = 250$		$V_0 = 500$		$V_0 = 1000$	
	$h_p/H = 0.1$	$h_p/H = 0.2$	$h_p/H = 0.1$	$h_p/H = 0.2$	$h_p/H = 0.1$	$h_p/H = 0.2$
0.1	1.0226	1.0194	1.0243	1.0206	1.0284	1.0236
0.2	1.0877	1.0755	1.0938	1.0801	1.1091	1.0914
0.4	1.3162	1.2753	1.3363	1.2909	1.3857	1.3284
0.8	1.9822	1.8723	2.0354	1.917	2.1634	2.0145
1	2.3616	2.217	2.4313	2.2729	2.5982	2.4038
1.5	3.6313	3.1319	3.4713	3.2209	3.7334	3.4279
2	4.3941	4.0817	4.5436	4.2028	4.8992	4.4848

the frequency ratio of FGO CNTRC plates. On contrary of pervious section, the variation of nonlinear elastic foundation affects the nonlinear response and all response curves exhibit hardening trend and increasing of K_{NL} yields the degree of hardening vary. Although, it should be noted that growth of K_{NL} results the increasing of frequency ratio.

In Fig. 9, the effect of piezoelectric layer thickness while applied voltage is zero, on frequency ratio is considered. In this case the total thickness of plate remains constant. According to the results, by increasing the thickness of piezoelectric layer, the degree of hardening is decreased. This behavior can be attributed from this fact, that by increasing the piezoelectric layer thickness, the amount of CNT through the thickness of plate is reduced and as result the stiffness of plate is decreased.

In Figs. 10 and 11, the effect of applying voltage on frequency ratio for $h_p/H = 0.1$ and 0.2 are shown, respectively. In this case, increasing applied voltage can vary the hardening type and growth its degree. It is cleared that by applying voltage the force and moment resultants due to the effect of piezoelectric layer are added to T_8 or linear parts of equation and as it is shown for linear elastic foundation parameter, increasing the linear parts of Eq. (23) results the reduction of frequency ratio. In Table 6, this matter is discussed in detail. As it is shown at the same applied voltage, increasing the thickness of piezoelectric layer results the reduction of hardening degree.

Fig. 12 depicts the effect of excitation force amplitude on W_{max}/h with different value of detuning parameter. The significance point in this figure is the jump phenomena for

$\sigma_1 > 1$. As it is shown, for the lowest value of force excited amplitude the jump phenomena has been occurred while with increasing the value of excitation force amplitude the steady state response is increased consequently.

Figs. 13 and 14 illustrate the influence of elastic foundation parameters on nonlinear response of CNTRC plate. According to these figures, increasing the value of linear elastic foundation results more stiffing behavior of CNTRC plate, but on contrary, rise in the nonlinear elastic foundation yields the softening response for CNTRC plate.

4. Conclusions

Nonlinear forced vibration of carbon nano-tube reinforcement of composite plates on nonlinear elastic foundation is evaluated using homotopy perturbation method. The classical plate theory with von Karman nonlinearity assumptions are employed to obtain the governing equations of the system. In this study the effects of various parameters including CNT volume fraction, elastic foundation and applied voltage on nonlinear response of CNTRC plates are considered. Based on the results, the elastic foundation parameters have significant roles in variation of steady state response. According to the obtained data, the effect of piezoelectric layer on nonlinear vibration behavior of functionally graded nanocomposite plate is more considerable in comparison to applied voltage.

References

Ansari, R. and Gholami, R. (2016), "Nonlinear primary resonance of third-order deformable functionally graded nanocomposite rectangular plates reinforced by carbon nanotubes", *Compos. Struct.*, **154**, 707-723.

Ansari, R., Faghih Shojaei, M., Mihammadi, V., Gholami, R. and Sadeghi, F. (2014), "Nonlinear forced vibration analysis of functionally graded carbon nanotube-reinforced composite Timoshenko beams", *Compos. Struct.*, **113**, 316-327.

Ansari, R., Hasrati, E., Faghih Shojaei, M., Gholami, R. and Shahbodini, A. (2015), "Forced vibration analysis of functionally graded carbon nanotube-reinforced composite plates using a numerical strategy", *Phys. E*: *Low-Dimens. Syst. Nanostruct.*, **69**, 294-305.

Ansari, R., Pourashraf, T., Gholami, R. and Shahbodini, A. (2016), "Analytical solution for nonlinear post buckling of functionally graded carbon nanotube-reinforced composite shells with piezoelectric layers", *Compos. Part B*: *Eng.*, **90**, 267-277.

Benedict, T. and Roy, T. (2016), "Vibration analysis of functionally graded carbon nano-tube-reinforced composite shell structures", *Acta Mech.*, **227**(2), 581-599.

Fazelzadeh, S.A., Pouresmaeeli, S. and Ghavanloo, E. (2015), "Aeroelastic characteristic of functionally graded carbon nano-tube-reinforced composite plates under a supersonic flow", *Comput. Meth. Appl. Mech. Eng.*, **285**, 714-729.

Gholami, R. and Ansari, R. (2017), "Large deflection geometrically nonlinear analysis of functionally graded multilayer graphene platelet-reinforced polymer composite rectangular plates", *Compos. Struct.*, **180**, 760-771.

Gholami, R. and Ansari, R. (2018) "Nonlinear harmonically excited vibration of third-order shear deformable functionally graded graphene platelet-reinforced composite rectangular plates", *Eng. Struct.*, **156**, 197-209.

Gholami, R., Ansari, R. and Gholami, Y. (2017) "Nonlinear resonant dynamics of geometrically imperfect higher-order shear deformable functionally graded carbon-nanotube reinforced composite beams", *Compos. Struct.*, **174**, 45-58.

Gorbanpour Arani, A. and Haghparast, E. (2017), "Vibration analysis of axially moving carbon nanotube reinforced composite plate under initial tension", *Polym. Compos.*, **38**(4), 814-822.

Gorbanpour Arani, A., Haghparast, E. and Babakbar Zaeri, H. (2017), "Vibration analysis of functionally graded nanocomposite plate moving in two directions", *Steel Compos. Struct.*, **23**(5), 529-541.

Gorbanpour Arani, A., Haghparast, E. and Babakbar, Z. (2016), "Vibration of axially moving 3-phase CNTFPC plate resting on orthotropic foundation", *Struct. Eng. Mech.*, **57**(1), 105-126.

Guo, X.Y. and Zhang, W. (2016), "Nonlinear vibrations of a reinforced composite plate with carbon nano-tubes", *Compos. Struct.*, **135**, 96-108.

He, J.H. (1999), "Homotopy perturbation technique", *Comput. Meth. Appl. Mech. Eng.*, **178**, 257-262.

Iijima, S.J. (1991), "Helical microtubules of graphitic carbon", *Nat.*, **354**, 56-58.

Ke, L.L., Yang, J. and Kitipornchai, S. (2010), "Nonlinear free vibration of functionally graded carbon nano-tube-reinforced composite beams", *Compos. Struct.*, **92**, 676-683.

Kiani, Y. (2016), "Free vibration of FG-CNT reinforced composite skew plates", *Aerosp. Sci. Technol.*, **58**, 178-188.

Kiani, Y. (2017), "Free vibration of FG-CNT reinforced composite spherical shell panels using Gram-Schmidt shape functions", *Compos. Struct.*, **159**, 368-381.

Kiani, Y. (2016), "Free vibration of functionally graded carbon nanotube reinforced composite plates integrated with piezoelectric layers", *Comput. Math. Appl.*, **72**(9), 2433-2449.

Memar Ardestani, M., Zhang, L.W. and Liew, K.M. (2017), "Isogeometric analysis of the effect of CNT orientation on the static and vibration behaviors of CNT-reinforced skew composite plates", *Comput. Meth. Appl. Mech. Eng.*, **317**, 341-379.

Mirzaei, M. and Kiani, Y. (2016), "Fee vibration of functionally graded carbon nanotube reinforced composite cylindrical panels, *Compos. Struct.*, **142**, 45-56.

Mirzaei, M. and Kiani, Y. (2016), "Free vibration of functionally graded carbon-nano-tube-reinforced composite plates with cutout", *Beilst. J. Nanotechnol.*, **7**(1), 511-523.

Rafiee, M., He, X.Q. and Liew, K.M. "Non-linear analysis of piezoelectric nanocomposite energy harvesting plates", *Smart Mater. Struct.*, **23**, 065001.

Ribeiro, P. (2016), "Non-local effects on the non-linear modes of vibration of carbon nano-tubes under electrostatic actuation", *Int. J. Non-Lin. Mech.*, **87**, 1-20.

Selim, B.A., Zhang, L.W. and Liew, K.M. (2017), "Active vibration control of CNT-reinforced composite plates with piezoelectric layers based on Reddy's higher-order shear deformation theory", *Compos. Struct.*, **163**, 350-364.

Selim, B.A., Zhang, L.W. and Liew, K.M. (2017), "Impact analysis of CNT-reinforced composite plates based on Reddy's higher-order shear deformation theory using an element-free approach", *Compos. Struct.*, **170**, 228-242.

Shams, S. and Soltani, B. (2016), "Buckling of laminated carbon nano-tube-reinforced composite plates on elastic foundations using a mesh free method", *Arab. J. Sci. Eng.*, **41**(5), 1981-1993.

Shen, H.S. (2012), "Thermal buckling and post buckling behavior of functionally graded carbon nano-tube-reinforced composite cylindrical shells", *Compos. Part B*: *Eng.*, **43**(3), 1030-1038.

Singh, G., Raju, K.K. and Rao, G.V. (1990), "Non-linear vibrations of simply supported rectangular cross-ply plates", *J.*

Sound Vibr., **142**, 213-226.

Wang, M., Li, Z.M. and Qiao, P. (2016), "Semi-analytical solutions to buckling and free vibration analysis of carbon nano-tube-reinforced composite thin plates", *Compos. Struct.*, **144**, 33-43.

Wang, Z.X. and Shen, H.S. (2012), "Nonlinear vibration and bending of sandwich plates with nano-tube-reinforced composite face sheets", *Compos. Part B*: *Eng.*, **43**(2), 411-421.

Wang, Z.X. and Shen, H.S. (2011), "Nonlinear vibration of nanotube-reinforced composite plates in thermal environments", *Comput. Mater. Sci.*, **50**, 2319-2330.

Zhang, L.W., Lei, Z.X., Liew, K.M. and Yu, J.L. (2014), "Large deflection geometrically nonlinear analysis of carbon nano-tube-reinforced functionally graded cylindrical panels", *Comput. Meth. Appl. Eng.*, **273**, 1-18.

Zhang, L.W., Song, Z.G., Qiao, P. and Liew, K.M. (2017), "Modeling of dynamic response of CNT-reinforced composite cylindrical shells under impact loads", *Comput. Meth. Appl. Mech. Eng.*, **313**, 889-903.

PL

Nomenclature

a	plate length
b	plate width
D	electrical displacement vector
e	piezoelectric matrix
E_m	matrix elastic modulus
E_p	piezoelectric elastic modulus
E	electrical field vector
G_m	host shear modulus
h	host thickness
h_p	piezoelectric layer thickness
H	total thickness of host and piezoelectric layer thickness
K_L	linear elastic stiffness foundation
K_{NL}	non-linear elastic stiffness foundation
p	embedding parameter
Q_{ij}	plane stress reduced stiffness
V_m	matrix volume fraction
V_{CN}	CNT volume fraction

V	applied voltage
σ	stress vector
ε	strain vector
ϵ	permittivity matrix
ρ_{CN}	CNT mass density
ρ_m	matrix mass density
ω_{CN}	SWCNTs mass fraction
v_{CN}	CNTs Poisson ratio
v_m	matrix Poisson ratio
α_m	matrix thermal expansion coefficient
$\alpha_{11}^{CN}, \alpha_{22}^{CN}$	CNTs thermal expansion coefficient

Appendix

$$T_1 = \left(\frac{m\pi}{a}\right)\left(\frac{n\pi}{b}\right)(A_{12} + A_{66})$$

$$T_2 = \left(\frac{m\pi}{a}\right)^2 A_{66} + \left(\frac{n\pi}{b}\right)^2 A_{22}$$

$$T_3 = \frac{-4}{9mn\pi^2}\left[\left(\frac{n\pi}{b}\right)^3 A_{22} + \left(\frac{m\pi}{a}\right)^2 \left(\frac{n\pi}{b}\right)(A_{12} - A_{66})\right]$$

$$T_4 = \left(\frac{m\pi}{a}\right)^2 A_{11} + \left(\frac{n\pi}{b}\right)^2 A_{66}$$

$$T_5 = \frac{-4}{9mn\pi^2}\left[\left(\frac{m\pi}{a}\right)^3 A_{11} + \left(\frac{n\pi}{b}\right)^2 \left(\frac{m\pi}{a}\right)(A_{12} - A_{66})\right]$$

$$T_6 = \left(\frac{m\pi}{a}\right)^4 D_{11} + 2\left(\frac{m\pi}{a}\right)^2 \left(\frac{n\pi}{b}\right)^2 (D_{12} + 2D_{66}) +$$
$$\left(\frac{n\pi}{b}\right)^4 D_{22} + 2V_0\left[e_{31}\left(\frac{m\pi}{a}\right)^2 + e_{32}\left(\frac{n\pi}{b}\right)^2\right] + K_L$$

$$T_7 = \frac{1}{16}\left\{\frac{9}{2}\left[\left(\frac{m\pi}{a}\right)^4 A_{11} + \left(\frac{n\pi}{b}\right)^4 A_{22}\right]\right.$$
$$\left. + \left(\frac{m\pi}{a}\right)^2 \left(\frac{n\pi}{b}\right)^2 (A_{12} + 2A_{66}) + 9K_{NL}\right\}$$